EAI Endorsed Transactions
on Scalable Information Systems
Research Article EAI.EU

Numerical Index Modulation Aided Multi-Carrier DCSK System: A Secure Transmission Scheme for Physical Layer Security

Wang Chen[1], Chao Duan[1,*]

[1]School of Information Engineering, Guangdong University of Bussiness and Technology

Abstract

This paper presents a novel Numerical Index Modulation-assisted Differential Chaos Shift Keying (NIM-DCSK) system, architected on a multi-carrier framework where numerous information-bearing subcarriers are supported by a single common reference subcarrier. The proposed system introduces an additional dimension for data transmission by embedding information bits into the dynamic allocation of signal energy across subcarriers. This mechanism not only boosts the transmission rate but also significantly enhances physical layer security. Specifically, the NIM-DCSK scheme obfuscates its transmission characteristics through pseudo-random energy allocation patterns, where deliberately varying power levels create a complex and non-stationary signal signature. This fluctuating energy distribution effectively masks the underlying data structure, making it extremely difficult for unauthorized eavesdroppers to perform feature analysis or achieve successful decoding. Compared to conventional DCSK systems, comprehensive analyses demonstrate that the NIM-DCSK system achieves substantial gains in both energy efficiency (EE) and spectral efficiency (SE), alongside improved bit error rate (BER) performance under various channel conditions. These advantages are realized without a commensurate increase in structural complexity. The inherent security features, including inherent resistance to passive interception and a reduced vulnerability to statistical analysis, are key benefits. Consequently, this work facilitates the integration of index modulation with chaos-based communications, ensuring high-rate transmissions coupled with robust security. The proposed system is, therefore, highly suitable for applications demanding reliable and secure wireless links, such as secure sensor networks, tactical military communications, and confidential IoT deployments.

Received on 15 September 2025; accepted on 19 October 2025; published on 25 February 2026

Keywords: Multi-carrier differential chaos shift keying, numerical index modulation, physical layer security.

doi:10.4108/eetsis.12043

1. Introduction

Nowadays, enhancing the reliability of wireless communication technologies has become one of the most pressing demands. Chaos theory, as a feasible scheme to improve reliability in the field of wireless communications, has attracted extensive research by numerous experts and scholars due to its effectiveness in ameliorating the communication transmission environment. As a crucial representation of chaos theory, chaotic signals possess unique properties such as sensitivity to initial conditions, randomness and unpredictability, broadband spectrum characteristics, and excellent auto-/cross-correlation properties. These attributes render chaotic signals highly applicable in the secure communications [1–3]. Chaotic signals can be utilized as carrier waves in spread spectrum communication, leveraging their wideband spectral properties to facilitate information transmission. Additionally, they can enhance system security through their pseudo-randomness and initial condition sensitivity.

Differential Chaos Shift Keying (DCSK), as one of the non-coherent schemes, has garnered widespread attention among researchers due to the lack of chaos synchronization and channel estimation. Consequently, current research on DCSK primarily concentrates

*Corresponding author. Email: duanchao@gzgs.edu.cn

on non-coherent demodulation scheme proposed by Kolumban [4]. Moreover, DCSK boasts advantages of low power consumption and high reliability, rendering it highly suitable for short-range wireless network scenarios such as wireless body area networks and wireless sensor networks [5, 6]. Despite these advantages, DCSK systems have some drawbacks including relatively low data transmission rates and energy efficiency. In traditional DCSK schemes, each data frame is divided into two slots: one for transmitting the reference signal and the other for the information-bearing signal. This approach results in a slower information transmission rate and considerable energy wastage. Furthermore, DCSK necessitates the use of radio frequency (RF) delay lines, complicating hardware implementation. To tackle these issues [7, 8], researchers have continuously developed optimized and improved DCSK schemes based on the original architecture. For instance, to enhance the reliability of DCSK systems, specifically BER performance, Kolumban et al. introduced frequency modulation DCSK (FM-DCSK) [9]. By employing frequency modulation, this scheme mitigates the issue of non-constant bit energy caused by the randomness of chaotic signals, thereby effectively improving system BER. Subsequently, an enhanced FM-DCSK system was proposed [10], which not only improved BER but also increased information transmission rates. Additionally, a noise reduction DCSK (NR-DSK) [11], was suggested to average the noise in reference signals, significantly enhancing BER performance maintaining low information transmission rates. [12], [13] present correlation delay shift keying (CDSK), a system transmitting mixed signals of reference and information-bearing components. While CDSK enhances information transmission rates and security by obscuring signal patterns from eavesdroppers, it also introduces cross-interference between signals, which negatively impacts BER performance.

To balance the preservation of BER advantage with improvements in information transmission rates and energy efficiency, short reference DCSK (SR-DCSK) has been proposed in [14], achieving higher data rates and energy efficiency without compromising BER by shortening bit durations. Enhanced DCSK schemes [15] and High-efficiency DCSK (HE-DCSK) [16] have also been designed to effectively increase data rates and energy efficiency. Furthermore, reference-modulated DCSK (RM-DCSK) [17] utilized reference signals as information-carrying elements, enhancing data rates while reducing the number of delay lines required in HE-DCSK systems. M-ary DCSK systems, designed based on M-ary constellations [18–21], represent another effective method for realizing high data rates and spectral efficiency by converting simple binary transmissions into multi-level symbol transmissions using constellation diagrams. Addressing the challenge of RF delay lines in DCSK systems, a code shifted DCSK (CS-DCSK) scheme has been proposed in [22]. This scheme eliminates the need for RF delay lines by leveraging the orthogonality of Walsh codes to distinguish between reference and information-bearing signals, enabling their simultaneous transmission and reducing system complexity. Kaddoum et al. extended DCSK systems into the frequency domain with multi-carrier DCSK (MC-DCSK) [23], conceptualized as a parallel expansion of RF delay circuit-free DCSK modulation. By transmitting reference and information-bearing signals via different frequency carriers and sharing a single reference signal among multiple information-bearing signals, MC-DCSK enhances information rates and bandwidth efficiency but increases system complexity.

With the rapid advancement of next-generation wireless communications, performance metrics have become increasingly diversified, with a particular emphasis on high speed and spectral efficiency. To meet these objectives, novel system designs combining various technologies with DCSK are essential to harness greater performance advantages. Existing technologies integrated with DCSK modulation include Index Modulation(IM) [24–27], spatial diversity [28], cooperative communication techniques [29], and channel coding [30].

Index Modulation (IM), an emerging technology proposed in recent years, has attracted significant research interest in next-generation wireless communications. The core principle of IM involves designing index rules based on existing system frameworks without directly altering waveforms. Instead, it selects different index sequences to convey information, thereby increasing information transmission rates. Index resources can be physical, such as antennas, subcarriers, time slots, frequencies, and spreading codes, or virtual, including signal constellations, space-time matrices, and antenna activation sequences. [31] pioneered the application of Code Index Modulation (CIM) in direct sequence spread spectrum communication systems, achieving high data transmission rates. Since then, research on combining IM techniques with DCSK systems has proliferated [31–35]. For example, [31] designed a novel CIM-assisted SR-DCSK system (CIM-DCSK), utilizing Walsh codes to carry additional information bits for high data rates. [32] proposed a hybrid modulation scheme combining pulse position modulation (PPM) and DCSK, exploiting time slots as indices to transmit extra information bits through slot activation patterns. In [33], a carrier index DCSK (CI-DCSK) scheme was introduced, activating different subcarriers to carry additional information bits based on their

active/inactive states. As research progressed, indexing methods evolved from single to multiple indices. [36] presented dual-mode modulation DCSK (DCSK-DIM) with index modulation, utilizing inactive and active time slots to transmit information bits, substantially increasing the data rate of PPM-DCSK schemes. A multidimensional index technique incorporating carriers, time slots, and orthogonal codes was applied to DCSK systems in [37], proposing a multidimensional-index-modulation DCSK (MIM-DCSK) scheme that significantly boosts data rates and spectral efficiency.

The integration of DCSK modulation with indexing technologies can significantly enhance communication system performance. However, this approach is still in the exploratory stage. Hence, this paper proposes proposes a numerical index modulation DCSK system to improve the BER performance, SE, EE as well as enhance the security. Simulation results reveal that the proposed NIM-DCSK scheme significantly enhances data rates compared to other DCSK schemes, improving energy and spectral efficiency while also yielding improvements in BER performance. For clarity, the main contributions of the paper can be summarized as follows:

1. The paper introduces a numerical index modulation DCSK (NIM-MC-DCSK) system, which is designed to carry additional information bits by leveraging numerical index rules within a multi-carrier framework. This innovation allows for the transmission of more data without compromising the inherent advantages of traditional DCSK systems.

2. A thorough analysis of the NIM-DCSK system's complexity, data rate, energy efficiency, and spectral efficiency is presented, highlighting its advantages over conventional DCSK systems.

3. Extensive simulation experiments were conducted to evaluate the impact of system parameters on Bit Error Rate (BER). These simulations confirmed the superior performance of the NIM-DCSK system compared to similar DCSK communication systems, demonstrating its enhanced reliability and robustness.

4. The results conclusively validate the effectiveness of the proposed NIM-DCSK scheme, showcasing significant improvements in BER performance and overall communication efficiency, thereby establishing its potential as a viable solution for advanced wireless communication applications.

The remainder of this paper is structured as follows: Section 2 introduces the system model of the proposed scheme. Section 3 and Section 4 analyze the performance metrics. Simulation results are presented in Section 5. Finally, Section 6 presents the conclusions of the paper.

2. System Model

The proposed NIM-MC-DCSK system shares a structural similarity with the CI-DCSK communication system. The system employs a total of $N+1$ subcarriers, consisting of one reference subcarrier and N information-bearing subcarriers, where N denotes the number of information-bearing subcarriers in the system. In the NIM-MC-DCSK system, a numerical indexing rule is designed to carry additional information bits. Under this scheme, information bits are not only mapped to the active/silent states of the subcarriers but also to the energy-level combinations utilized by the activated subcarriers.

2.1. Transmitter Structure

Figure 1 illustrates the transmitter structure of the NIM-MC-DCSK system. A chaotic signal generator produces a chaotic sequence, which is then shaped by a pulse-shaping filter to form the reference signal and transmitted via a carrier with a center frequency of f_c. Given that the length of the reference signal is L, the generated chaotic reference signal can be expressed as:

$$c(t) = \sum_{k=1}^{L} c_k h(t - kT_c), \tag{1}$$

Meanwhile, the information-bearing signals are transmitted through the remaining N subcarriers at different frequencies. Assume that within one symbol duration, the NIM-MC-DCSK system transmits a total of P information bits, which consist of index bits and modulation bits. The index bits are further divided into subcarrier index bits and numerical index bits. The subcarrier index bits select one subcarrier from the N subcarriers to remain silent, while the remaining $N-1$ subcarriers are activated. There are N possible selection cases. Therefore, the number of subcarrier index bits is calculated as $p_1 = log_2^N$ The numerical index bits determine the energy allocation among the $N-1$ activated subcarriers. Specifically, one subcarrier is selected to have energy β, while the remaining $N-2$ activated subcarriers have energy α, where $\beta > \alpha > 0$. This gives $N-1$ possible selection cases. Thus, the number of numerical index bits is calculated as $p_2 = \left\lfloor \log_2^{N-1} \right\rfloor$, where $\lfloor(\cdot)\rfloor$ denotes the floor operations. The modulation bits are carried by the polarities of the $N-1$ activated subcarriers, giving as $p_3 = N-1$. Therefore, the total number of transmitted information bits per symbol is $p = p_1 + p_2 + p_3$. For clarity, Table 1 provides an example of the index mapping rules when $N = 4$ information-bearing subcarriers are used. In this case,

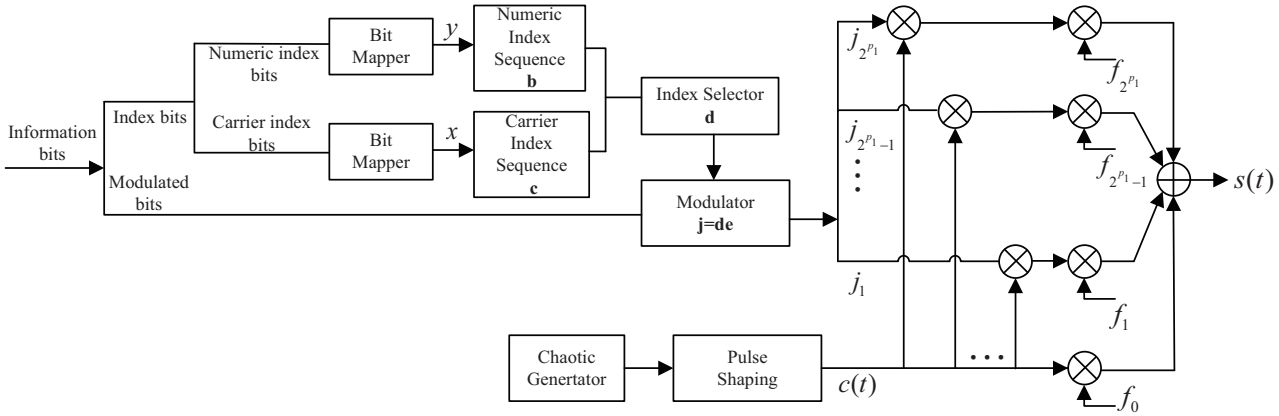

Figure 1. Transmitter architecture of the NIM-MC-DCSK system

Table 1. Energy Allocation Schemes and Index Bit Mapping

Energy Allocation	Activated Subcarriers	Energy Matrix	Subcarrier Index Bits	Numerical Index Bits
Scheme 1	{1,2,3}	$\mathbf{d} = [\beta, \alpha, \alpha, 0]$	00	0
	{1,2,4}	$\mathbf{d} = [\beta, \alpha, 0, \alpha]$	01	0
	{1,3,4}	$\mathbf{d} = [\beta, 0, \alpha, \alpha]$	10	0
	{2,3,4}	$\mathbf{d} = [0, \beta, \alpha, \alpha]$	11	0
Scheme 2	{1,2,3}	$\mathbf{d} = [\alpha, \beta, \alpha, 0]$	00	1
	{1,2,4}	$\mathbf{d} = [\alpha, \beta, 0, \alpha]$	01	1
	{1,3,4}	$\mathbf{d} = [\alpha, 0, \beta, \alpha]$	10	1
	{2,3,4}	$\mathbf{d} = [0, \alpha, \beta, \alpha]$	11	1
Scheme 3	{1,2,3}	$\mathbf{d} = [\alpha, \alpha, \beta, 0]$	N/A	N/A
	{1,2,4}	$\mathbf{d} = [\alpha, \alpha, 0, \beta]$	N/A	N/A
	{1,3,4}	$\mathbf{d} = [\alpha, 0, \alpha, \beta]$	N/A	N/A
	{2,3,4}	$\mathbf{d} = [0, \alpha, \alpha, \beta]$	N/A	N/A

the numbers of subcarrier index bits and numerical index bits can be calculated as 2 and 1 respectively, i.e., $p_1 = 2$ and $p_1 = 1$. Taking the second row of the second energy allocation scheme in Table 1 as an example.when the subcarrier index bits are "01" and the numerical index bit is "1", the subcarrier at position 3 is not activated and remains de-activated, while among the remaining three activated subcarriers f_1, f_2 and f_4, the subcarrier at the numerically indexed position 2 has energy β, and the other activated subcarriers have energy α. The modulation bits are then transmitted using these three activated subcarriers.

We also present the signal frame structure of the information-bearing subcarriers, as shown in Figure 2. It can be observed that subcarrier 3 remains in a de-activated state, and subcarrier 2 carries an energy value of β. The remaining subcarriers f_1 and f_4 each carry an energy value of α. Based on the activated subcarrier positions and energy matrix in Table 1, we can deduce that the transmitted index bits and numerical index bits for this signal frame are "01" and "1", respectively.

Specifically, the subcarrier index bits and numerical index bits are mapped through a bit mapper to obtain the combination (x, y), where x and y represent the position indices of the silent subcarrier and the subcarrier with maximum energy, respectively. Therefore, the energy matrix of the information-bearing signal can be expressed as either $\mathbf{d} = [\alpha_1, \alpha_2 \cdots, 0_x, \cdots, \beta_y, \cdots \alpha_N]^T$ or $\mathbf{d} = [\alpha_1, \alpha_2 \cdots, \beta_y, \cdots, 0_x, \cdots \alpha_N]^T$, where $x, y = 1, 2 \cdots N$ and $x \neq y$. The index selector needs to generate such an energy matrix based on the relationship between x and y derived from the index bit mapping, which is then fed into the modulator.

Within the modulator, the $N-1$ modulation bits transmitted during one symbol period are mapped to an information matrix $\mathbf{e} = [e_1, e_2, \cdots, e_i, \cdots, e_{N-1}]^T, (i = 1, 2, \cdots, N-1)$, which constitutes an $N-1$-dimensional row vector matrix. When a modulation bit is '1', the corresponding element $e_i = +1$; when the modulation bit is '0', $e_i = -1$. Each element in the information matrix is then multiplied with the $N-1$ activated subcarriers through dot product operations, thereby utilizing the polarity of the activated subcarriers to carry the modulation bits. In essence, this process embeds the modulation information onto the signals of these $N-1$ activated

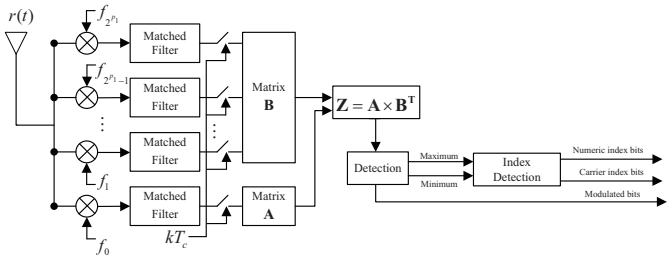

Figure 2. Receiver architecture of the NIM-DCSK system

subcarriers, which are subsequently transmitted together with the index bits.

2.2. Receiver Structure

Figure 2 shows the block diagram of the designed NIM-MC-DCSK receiver structure. The main working principle is analyzed as follows: The received signal $r(t)$ is multiplied by sinusoidal carriers of different frequencies and then filtered t hrough m atched filters. At each time instant kT_c, the product signals are sampled and stored in matrices A and B. Here, the chaotic reference signal is represented by matrix $A^{1\times R}$, while the data information is stored in matrix $B^{N\times R}$. Next, we perform a correlation operation between the reference signal matrix A and matrix B to obtain the information signal matrix $Z^{1\times N}$ and input it into the energy detector. The correlation matrix is calculated as follows:

$$\mathbf{Z} = \mathbf{A} \times \mathbf{B}^T = [Z_1, \cdots, Z_N] \tag{2}$$

In the energy detector, we take the absolute values of all elements in the information signal matrix Z, obtaining a total of N element values. By comparing these Z values, we identify the positions of the minimum and maximum values to perform index detection and recover the information bits. The restored index of the silent subcarrier and the numerical index among the active subcarriers can be expressed as:

$$\hat{x} = \arg \min_{i=1,\ldots,N} (|Z_i|) \tag{3}$$

$$\hat{y} = \arg \max_{i=1,\ldots,N} (|Z_i|) \tag{4}$$

where $\hat{x}$ and $\hat{y}$ are the estimated symbols for subcarrier index and numerical index, respectively.

The corresponding index bits are recovered based on the positional relationship between the minimum $\hat{x}$ and maximum value $\hat{y}$ locations, with specific mapping rules detailed in Table 1. Notably, since certain energy allocation schemes remain unused during transmission, the recovery process may occasionally yield estimates corresponding to these unused configurations. In such cases, the index detector will randomly select from equally probable bit combinations for recovery. It should be emphasized that an error in subcarrier index recovery may propagate to affect numerical index estimation, as these two recovery processes exhibit mutual dependence. Regarding modulation bit recovery, the element at position *hatx* is first removed from the information signal matrix Z, after which the remaining $N-1$ elements undergo polarity detection to estimate the modulation bits.

3. Performance Analysis

3.1. Data Rate and Complexity Analysis

In conventional analysis of DCSK systems, the data rate is typically defined as the ratio of the total number of transmitted bits per symbol to the symbol duration [63]. For the NIM-MC-DCSK system, the subcarrier index and numerical index carry additional log_2^N and $\left\lfloor \log_2^{N-1} \right\rfloor$ information bits, respectively, where $\left\lfloor \log_2^{N-1} \right\rfloor = \log_2^N - 1$, combined with $N-2$ modulation bits, resulting in a total information bit count of $N - 2 + 2\log_2^N$ per symbol. Given that the designed NIM-MC-DCSK system employs a symbol duration of LT_c, the data rate of the proposed system can be expressed as $\frac{N-2+2\log_2^N}{LTc}$.

Meanwhile, we conducted a comparative analysis of data rates for other DCSK systems using the same methodology. The CIM-MC-DCSK system [64] employs Walsh codes to process the reference signal, thereby carrying additional index bits. Consequently, its data rate becomes $\frac{\log_2^P + N\log_2^M}{LTc}$, where P denotes the order of Walsh codes and $P = N$, and L represents the modulation order. The date rate of the other CI-DCSK, MC-DCSK and Conventional DCSK systems are $\frac{N-1+\log_2^N}{LTc}$, $\frac{N}{LTc}$, and $\frac{1}{LTc}$, respectively.

As detailed in Table 2, the proposed NIM-MC-DCSK system achieves superior performance by transmitting significantly m ore i nformation b its w ithin t he same symbol duration, yielding a substantially enhanced data rate compared to benchmark systems.

Table 2. Comparison of Data Rates Among Different DCSK Systems

System	Data Rate
NIM-DCSK	$\frac{N-2+2\log_2^N}{LTc}$
CIM-MC-DCSK	$\frac{\log_2^P + N\log_2^M}{LTc}$
MC-DCSK	$\frac{N}{LTc}$
CI-DCSK	$\frac{N-1+\log_2^N}{LTc}$
DCSK	$\frac{1}{LTc}$

This section analyzes and discusses the complexity of various DCSK systems. Generally, the complexity study of DCSK schemes involves two main components: 1) the complexity of spreading/despreading operations, and 2) the complexity of index search, defined a s the number of comparison operations required to detect inactive subcarriers and identify different energy levels among active subcarriers. In the proposed system, similar to subcarrier index modulation approaches, it requires generating a L length chaotic reference signal. Therefore, the spreading/despreading complexity is $\mathcal{O}(NL)$, the index search complexity is $\mathcal{O}(C_N^1 + C_{N-1}^1)$, as the system must identify one inactive subcarrier among N candidates, and perform energy level detection across $N-1$ active subcarriers. Thus, the total system complexity can be expressed as $\mathcal{O}(NL + C_N^1 + C_{N-1}^1)$. For fair comparison, we also analyze the complexity of CIM-MC-DCSK, MC-DCSK, CI-DCSK, and conventional DCSK systems, as detailed in Table 3.

Table 3. Comparison of Computational Complexity Among DCSK Systems

System	Complexity
NIM-MC-DCSK	$\mathcal{O}(NL + C_N^1 + C_{N-1}^1)$
CIM-MC-DCSK	$\mathcal{O}((2N + PN)\,\vartheta + C_P^1)$
MC-DCSK	$\mathcal{O}(N+1)$
CI-DCSK	$\mathcal{O}(NL + C_N^1)$
DCSK	$\mathcal{O}(2L)$

To provide a more intuitive performance comparison, we systematically evaluate the computational complexity per transmitted bit versus spreading factor relationship across different DCSK architectures under standardized testing conditions. For equitable comparison, all systems are configured to transmit 6 bits per symbol through specific parameter selections. The NIM-MC-DCSK system employs $N = 5$ subcarriers, CIM-MC-DCSK utilizes Walsh code order $K = 4$ with modulation order $L = 2$, while both MC-DCSK and CI-DCSK adopt $N = 7$ subcarriers. It should be noted that certain inherent limitations prevent some systems from achieving identical configurations particularly, neither CI-DCSK nor conventional DCSK can reach the target 6 bits per symbol under normal operational parameters. This normalized comparison framework enables meaningful cross-system evaluation while accounting for each architecture fundamental constraints, with the subsequent analysis demonstrating how the proposed NIM-MC-DCSK maintains superior complexity efficiency across practical spreading factor ranges despite these implementation challenges. The results reveal consistent performance advantages even when compensating for different systems native bit-carrying capacities through careful parameter selection.

3.2. Energy Efficiency and Spectral Efficiency Analysis

In conventional performance metrics, energy efficiency (EE) is defined as the ratio of transmitted bits per symbol to symbol energy, while spectral efficiency (SE) represents the ratio of data rate to total bandwidth. We systematically evaluate these metrics for the NIM-MC-DCSK system and benchmark systems with detailed results presented in Figure 3 and Figure 4. Without loss of generality, we assume $E_c = 1$, and ψ is subcarrier bandwidth (in Hz). As shown in Figure 3, we analyze

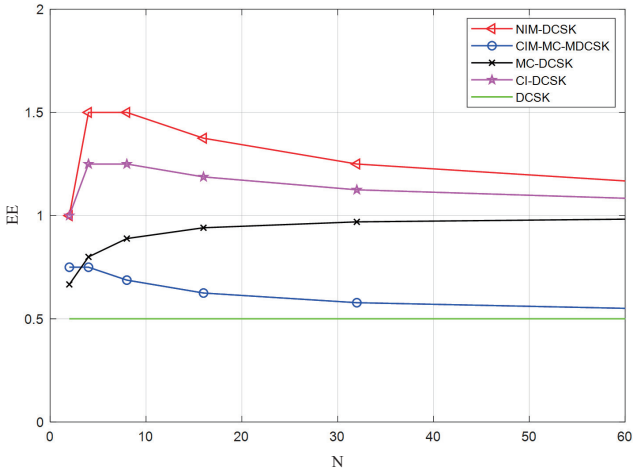

Figure 3. EE of the NIM-MC-DCSK system

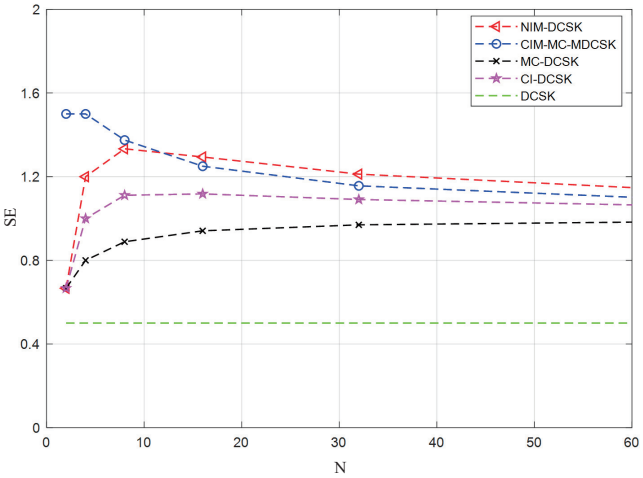

Figure 4. SE of the NIM-MC-DCSK system

the relationship between various DCSK systems and the spreading factor L. With increasing L, the NIM-MC-DCSK and CI-DCSK systems maintain similar computational complexity, while the NIM-MC-DCSK system transmits significantly m ore i nformation bits. Compared to other systems such as CIM-MC-DCSK and MC-DCSK, the NIM-MC-DCSK system demonstrates notably lower complexity.

Comparative analysis reveals that while existing multi-index DCSK systems employing orthogonal codes and Hilbert transforms achieve moderate transmission efficiency improvements, they incur substantially higher computational complexity. Conversely, conventional low-complexity DCSK architectures demonstrate inadequate resource utilization, resulting in limited data rates. The proposed system achieves an optimal balance, maintaining low computational complexity while significantly enhancing the data rate.

Figure 4 compares the energy efficiency versus number of subcarriers for NIM-DCSK, CIM-MC-MDCSK, MC-DCSK, CI-DCSK, and conventional DCSK systems. The results demonstrate that the proposed NIM-DCSK system achieves superior energy efficiency across the evaluated subcarrier range, particularly showing significant advantages when the number of subcarriers exceeds 15. The performance gap between NIM-DCSK and other systems progressively widens with increasing subcarrier count, highlighting the scalability of our design.

The superior performance stems from the system's innovative design which effectively balances computational complexity with transmission efficiency, as evidenced by the quantitative comparisons presented in previous sections. The experimental data validate NIM-DCSK's ability to simultaneously optimize both efficiency parameters without compromising practical implementability.

4. Simulation Results

This section analyzes the BER performance of the proposed system. We conducted Monte Carlo simulations to verify the BER advantages of the NIM-MC-DCSK system under both AWGN and multipath Rayleigh fading channels. For the Rayleigh fading channel model, we considered three propagation paths with equal power gain $E[\lambda_1^2] = E[\lambda_2^2] = E[\lambda_3^2] = 1/3$ and path delays of $\tau_1 = 0, \tau_1 = 1$, and $\tau_2 = 2$ chip intervals. We first analyze the BER performance of the NIM-MC-DCSK system under different parameter configurations, taking the number of subcarriers $N = 16$ and the reference signal length $L = 80$ as examples. By assigning different values to α and β, we conduct simulation experiments under both AWGN and multipath Rayleigh fading channels, as shown in Figure 5. The experimental results reveal that when $\alpha = 0.5, \beta = 2$, the system achieves the optimal BER performance among all tested parameter configurations. This is because the parameter selection must balance the trade-off between the error probability of index detection and the optimization of system SNR. If the ratio of α and β is too small, the error probability of identifying the maximum energy subcarrier increases significantly. Conversely, if α and β is too large, the error probability of detecting the minimum energy

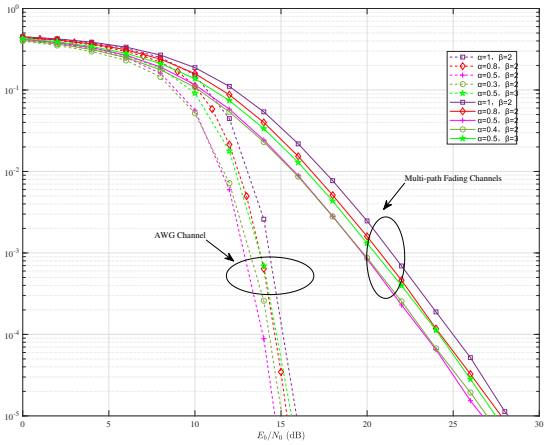

Figure 5. BER of the NIM-MC-DCSK system over different α and β

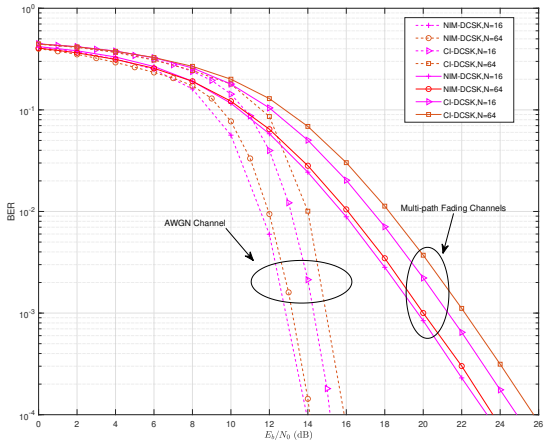

Figure 6. BER of the NIM-MC-DCSK system compared with the CI-DCSK system

subcarrier also rises, both of which adversely affect the recovery of index bits. Experimental results confirm that $\alpha = 0.5, \beta = 2$ not only ensures low error probability in subcarrier index detection but also maintains high reliability in numerical index recognition, thereby achieving optimal overall BER performance. Unless otherwise specified, a ll s ubsequent s imulations adopt $\alpha = 0.5, \beta = 2$. Secondly, we investigate the impact of reference signal length L on BER performance. Taking $N = 8$ as an example, we analyze the BER under multipath Rayleigh fading channels with SNR values of 12 dB, 16 dB, and 20 dB, as illustrated in Figure 6. The results demonstrate that as L increases, the system performance initially improves due to enhanced autocorrelation and cross-correlation properties of the chaotic reference sequence. The BER reaches its optimal point at a specific reference length L_{opt}, beyond which further increasing L degrades performance. This degradation occurs because longer reference sequences incorporate more noise components, ultimately deteriorating the

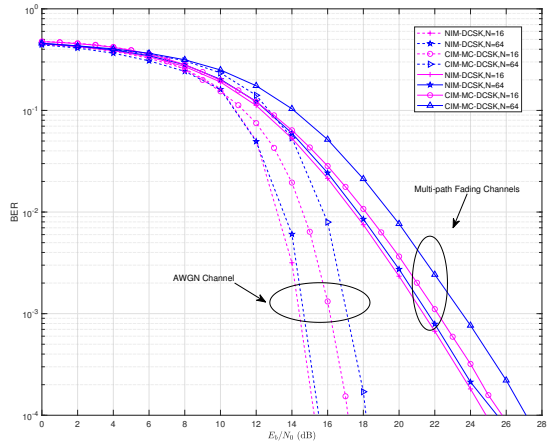

Figure 7. BER of the NIM-MC-DCSK system compared with the CIM-DCSK system

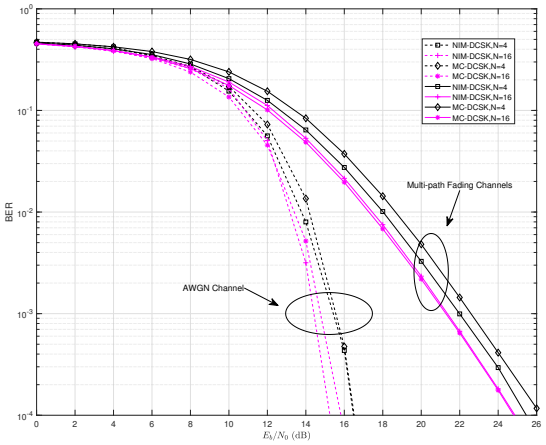

Figure 8. BER of the NIM-MC-DCSK system compared with the MC-DCSK system

overall BER. The experimental data confirm the existence of an optimal operating point that balances correlation properties against noise accumulation effects. We then compare the BER performance between the NIM-MC-DCSK system and other DCSK systems. Figure 7 shows the BER comparison between NIM-MC-DCSK and CIM-MC-MDCSK systems, where the NIM-DCSK system uses spreading factors $L = 256$ and $N = 16$ and 64 for information-bearing subcarriers. For fair comparison, the CIM-MC-MDCSK system adopts identical parameter settings with modulation order $L = 2$. In the figure, d ashed l ines r epresent A WGN c hannel conditions while solid lines indicate multipath Rayleigh fading channels. The results demonstrate that under these configurations, t he N IM-MC-DCSK s ystem achieves superior BER performance to CIM-MC-MDCSK in both channel models. For instance, in AWGN channel with same parameters, the proposed NIM-MC-DCSK system provides 1.5-2 dB performance improvement at BER of 10^{-3} compared to CIM-MC-MDCSK. Similar performance advantages are observed under fading channel conditions as well. These experimental results validate that NIM-MC-DCSK maintains better error rate characteristics while preserving its complexity and efficiency advantages discussed in previous sections. Figure 8 compares the BER performance between NIM-DCSK and MC-DCSK systems with spreading factor L and information-bearing subcarrier numbers $N = 4$ and 16. The dashed lines represent AWGN channel conditions while solid lines indicate multipath Rayleigh fading channels. Results show that under identical parameter settings, NIM-MC-DCSK achieves comparable BER performance to MC-DCSK in both channel models. This demonstrates that with the same subcarrier resources, NIM-MC-DCSK maintains similar error rate performance while carrying more information bits than MC-DCSK. As shown in Figure 9, we compare the BER

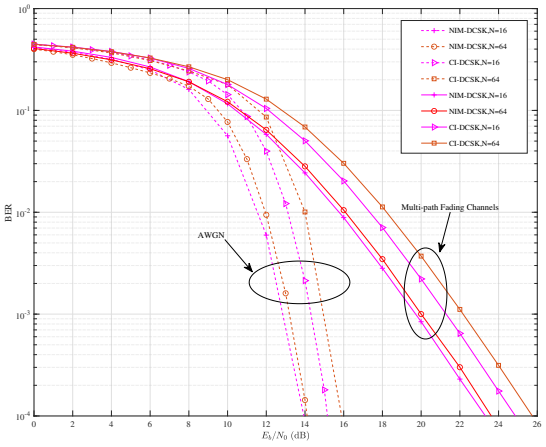

Figure 9. BER of the NIM-MC-DCSK system compared with the CI-DCSK system

performance between the NIM-DCSK system and CI-DCSK system. The spreading factor is set to 80 with information-bearing subcarrier numbers of 16 and 64. In the figure, d ashed l ines r epresent A WGN channel conditions while solid lines indicate multipath Rayleigh fading channels. The results show that the NIM-MC-DCSK system achieves better BER performance than CI-DCSK under both channel models.

Specifically, i n t he A WGN c hannel a t 1 4dB with $N = 26$, the proposed NIM-DCSK system achieves a BER of 10^{-4}, while the CI-DCSK system only reaches approximately 10^{-2}. Under multipath Rayleigh fading channel at 24dB with $N = 64$, the BER of the NIM-MC-DCSK system remains well below 10^{-4}, whereas the BER of the CI-DCSK system falls within the range of 10^{-2} to 10^{-3} . These results clearly demonstrate that the NIM-MC-DCSK system exhibits superior BER performance compared to the CI-DCSK system.

5. Conclusion

We propose a numerical index-assisted DCSK system (NIM-MC-DCSK) that simultaneously enhances both communication performance and security characteristics. The novel indexing scheme's dynamic energy allocation patterns introduce additional security dimensions by making signal characteristics less predictable to potential eavesdroppers. Comprehensive evaluations demonstrate the system's advantages in computational complexity, data rate, and error performance while establishing its inherent security benefits through chaotic signal properties combined with index randomization. The proposed architecture provides a foundation for developing secure chaotic communication systems that meet both performance and security requirements of next-generation wireless networks.

Authors' Contributions

Conceptualization: W.C.; Methodology, W.C. software, W.C.; validation, C.D.; formal analysis, C.D.; investigation, W.C.; resources, C.D.; data curation, W.C.; writing—original draft preparation, W.C.; writing—review and editing, C.D.; visualization, W.C.; supervision, C.D.; project administration, C.D.; funding acquisition, C.D. All authors have read and agreed to the published version of the manuscript.

Funding

This work was supported by Guangzhou College of Technology and Business Quality Engineering Project (YLZY202301, KCJYS202404); Foshan City Self-financed Scientific and Technological Innovation Projects (2420001004716).

Availability of Data and Material

The data sets used and analyzed during the current study are available from the corresponding authors on reasonable request.

Acknowledgements

No.

Conflict of Interest

The authors declare that they have no potential conflict of interest with respect to the research, authorship and publication of this article.

Ethical approvals

Not applicable.

References

[1] G. Mazzini, G. Setti, and R. Rovatti, "Chaotic complex spreading sequences for asynchronous DS-CDMA. I. System modeling and results,"*IEEE Trans. Circuits Syst. I, Fundam. Theory Appl.*, vol. 44, no. 10, pp. 937-947, Oct. 1997.

[2] A. P. Kurian, S. Puthusserypady, and M. H. Su, "Performance enhancement of DS/CDMA system using chaotic complex spreading sequence,"*IEEE Trans. Wireless Commun.*, vol. 4, no. 3, pp. 984-989, Mar. 2005.

[3] H. Dedieu, M. P. Kennedy, and M. Hasler, "Chaos shift keying: Modulation and demodulation of a chaotic carrier using self-synchronizing Chua's circuits,"*IEEE Trans. Circuits Syst. II, Analog Digit. Signal Process.*, vol. 40, no. 10, pp. 634-642, Oct. 1993.

[4] G. Kolumbán, B. Vizvári, W. Schwarz, and A. Abel, "Differential chaos shift keying: A robust coding for chaos communication," *in Proc. NDES*, 1996, pp. 87-92.

[5] C. C. Chong and S. K. Yong, "UWB direct chaotic communication technology for low-rate WPAN applications,"*IEEE Trans. Veh. Technol.*, vol. 57, no. 3, pp. 1527-1536, Mar. 2008.

[6] G. Cai, Y. Fang, J. Wen, L. Wang, and G. Chen, "QoS-aware buffer-aided relaying implant WBAN for healthcare IoT: Opportunities and challenges,"*IEEE Netw.*, vol. 33, no. 4, pp. 96-103, Jul. 2019.

[7] G. Kolumbán, G. Kis, M. P. Kennedy, and Z. Jákó, "FM-DCSK: A new and robust solution to chaos communications," *in Proc. Int. Symp. Nonlinear Theory Appl.*, 1997, pp. 1-6.

[8] G. Kaddoum and E. Soujeri, "NR-DCSK: A noise reduction differential chaos shift keying system,"*IEEE Trans. Circuits Syst. II, Exp. Briefs*, vol. 63, no. 7, pp. 648-652, Jul. 2016.

[9] J. H. Lee and H. G. Ryu, "A new receiver design of CDSK-based chaos communication system," *in Proc. ICTC*, 2013.

[10] M. Sushchik, L. S. Tsimring, and A. R. Volkovskii, "Performance analysis of correlation-based communication schemes utilizing chaos,"*IEEE Trans. Circuits Syst. I, Fundam. Theory Appl.*, vol. 47, no. 12, pp. 1684-1691, Dec. 2000.

[11] G. Kaddoum, E. Soujeri, and Y. Nijsure, "Design of a short reference noncoherent chaos-based communication system,"*IEEE Trans. Commun.*, vol. 64, no. 2, pp. 680-689, Feb. 2016.

[12] G. Kolumbán, Z. Jákó, M. P. Kennedy, and L. Kis, "Enhanced versions of DCSK and FM-DCSK data transmission systems," *in Proc. ISCAS*, 1999.

[13] H. Yang and G. P. Jiang, "High-efficiency differential-chaos-shift-keying scheme for chaos-based noncoherent communication,"*IEEE Trans. Circuits Syst. II, Exp. Briefs*, vol. 59, no. 5, pp. 312-316, May 2012.

[14] H. Yang and G. P. Jiang, "Reference-modulated DCSK: A novel chaotic communication scheme,"*IEEE Trans. Circuits Syst. II, Exp. Briefs*, vol. 60, no. 4, pp. 232-236, Apr. 2013.

[15] L. Wang, G. Cai, and G. Chen, "Design and performance analysis of a new multiresolution M-ary differential chaos shift keying communication system,"*IEEE Trans. Wireless Commun.*, vol. 14, no. 9, pp. 5197-5208, Sep. 2015.

[16] G. Cai, Y. Fang, G. Han, L. Wang, and G. Chen, "A square-constellation-based M-ary DCSK communication system,"*IEEE Access*, vol. 4, pp. 6295-6303, 2016.
[17] G. Cai, Y. Fang, and G. Han, "Design of an adaptive multiresolution M-ary DCSK system,"*IEEE Commun. Lett.*, vol. 21, no. 1, pp. 60-63, Jan. 2017.
[18] W. Xu, L. Wang, and G. Chen, "Performance analysis of the CS-DCSK/BPSK communication system,"*IEEE Trans. Circuits Syst. I, Reg. Papers*, vol. 61, no. 9, pp. 2624-2633, Sep. 2014.
[19] G. Kaddoum, F. D. Richardson, and F. Gagnon, "Design and analysis of a multi-carrier differential chaos shift keying communication system,"*IEEE Trans. Commun.*, vol. 61, no. 8, pp. 3281-3291, Aug. 2013.
[20] E. Basar, M. Wen, R. Mesleh, M. Di Renzo, Y. Xiao, and H. Haas,"Index modulation techniques for next-generation wireless networks,"*IEEE Access*, vol. 5, pp. 16693-16746, 2017.
[21] M. C. Gursoy, E. Basar, A. E. Pusane, and U. Aygolu, "Index modulation for molecular communication via diffusion systems,"*IEEE Trans. Commun.*, vol. 67, no. 5, pp. 3337-3350, May 2019.
[22] M. Wen, E. Basar, Q. Li, B. Zheng, and M. Zhang, "Multiple-mode orthogonal frequency division multiplexing with index modulation,"*IEEE Trans. Commun.*, vol. 65, no. 9, pp. 3892-3906, Sep. 2017.
[23] Q. Li, M. Wen, E. Basar, H. V. Poor, and B. Zheng, "Index modulated OFDM spread spectrum,"*IEEE Trans. Wireless Commun.*, vol. 17, no. 4, pp. 2360-2374, Apr. 2018.
[24] R. Liu, "Cooperative communications and networking (Liu, K.J.R. et al) [Book Review],"*IEEE Signal Process. Mag.*, vol. 26, no. 5, pp. 149-150, Sep. 2009.
[25] Y. Fang, P. Chen, G. Cai, L. Wang, and G. Chen, "Outage-limit-approaching channel coding for future wireless communications: Root-protograph low-density parity-check codes,"*IEEE Veh. Technol. Mag.*, vol. 14, no. 2, pp. 85-93, Jun. 2019.
[26] G. Kaddoum, M. F. A. Ahmed, and Y. Nijsure, "Code index modulation: A high data rate and energy efficient communication system,"*IEEE Commun. Lett.*, vol. 19, no. 2, pp. 175-178, Feb. 2015.
[27] X. Cai, W. Xu, F. C. M. Lau, S. Wang, and G. Chen, "Joint carrier-code index modulation aided M-ary differential chaos shift keying system,"*EEE Trans. Veh. Technol.*, vol. 69, no. 12, pp. 15486-15499, Dec. 2020.
[28] H. Ma, G. Cai, Y. Fang, P. Chen, and G. Chen, "Design of a superposition coding PPM-DCSK system for downlink multi-user transmission,"*IEEE Trans. Veh. Technol.*, vol. 69, no. 2, pp. 1666-1678, Feb. 2020.
[29] S. Liu, P. Chen, and G. Chen, "Differential permutation index DCSK modulation for chaotic communication system,"*IEEE Commun. Lett.*, vol. 25, no. 6, pp. 2029-2033, Jun. 2021.
[30] W. Xu, T. Huang, and L. Wang, "Code-shifted differential chaos shift keying with code index modulation for high data rate transmission,"*IEEE Trans. Commun.*, vol. 65, no. 10, pp. 4285-4294, Oct. 2017.
[31] W. Xu, Y. Tan, F. C. M. Lau, and Y. Guan, "Design and optimization of differential chaos shift keying scheme with code index modulation,"*IEEE Trans. Commun.*, vol. 66, no. 5, pp. 1970-1980, May 2018.
[32] M. Miao, L. Wang, M. Katz, and G. Chen, "Hybrid modulation scheme combining PPM with differential chaos shift keying modulation,"*IEEE Wireless Commun. Lett.*, vol. 8, no. 2, pp. 340-343, Apr. 2019.
[33] G. Cheng, L. Wang, W. Xu, and G. Chen, "Carrier index differential chaos shift keying modulation,"*IEEE Trans. Circuits Syst. II, Exp. Briefs*, vol. 64, no. 8, pp. 907-911, Aug. 2017.
[34] Y. Tao, Y. Fang, H. Ma, P. Chen, and G. Chen, "Multi-carrier DCSK with hybrid index modulation: A new perspective on frequency-index-aided chaotic communication,"*IEEE Trans. Commun.*, vol. 70, no. 6, pp. 3760-3773, Jun. 2022.
[35] Y. Fang, J. Zhuo, H. Ma, P. Chen, and G. Chen, "Design and analysis of a new index-modulation-aided DCSK system with frequency-and-time resources,"*IEEE Trans. Veh. Technol.*, vol. 72, no. 1, pp. 237-256, Jan. 2023.
[36] X. Cai, W. Xu, S. Hong, F. C. M. Lau, and G. Chen, "Dual-mode differential chaos shift keying with index modulation,"*IEEE Trans. Commun.*, vol. 67, no. 9, pp. 6099-6111, Sep. 2019.
[37] H. Ma, Y. Fang, P. Chen, and G. Chen, "A novel differential chaos shift keying scheme with multidimensional index modulation,"*IEEE Trans. Wireless Commun.*, vol. 22, no. 1, pp. 237-256, Jan. 2023.